Photosynthetic CO_2 uptake by terrestrial vegetation from coupled CO_2-COS flux measurements

David Asaf[1], Eyal Rotenberg[1], Uri Dicken[1], Fyodor Tatarinov[1], Steve Montzka[2] & Dan Yakir[1]*

[1]Environmental Sciences and Energy Research, Weizmann Instiute of Science, Rehovot 76100, Israel. [2]NOAA-ESRL, Boulder, CO 80305, USA.

The rate of increase in atmospheric CO_2 concentration is only about half of that expected based on rates of fossil fuel emissions (1,2). The ocean and the land biosphere must absorb the CO_2 not accumulated in the atmosphere. On land, our understanding of CO_2 sinks and sources is limited by the inability to distinguish between CO_2 uptake in photosynthetic gross primary productivity (GPP) and release in respiration. Recent studies have suggested the utility of carbonyl sulfide (COS) uptake as a powerful new proxy for GPP based on the close relationship between COS and CO_2 at regional, local and leaf scales (3-9). Here, we directly test the COS/CO_2 approach using eddy covariance and laser spectroscopy (10) to estimate net exchange of CO_2 (NEE) and COS (F_{cos}). GPP is then estimated directly from F_{cos} and indirectly from NEE (11) with good agreement: 657±230 vs. 578±220 mmol CO_2 m^{-2} d^{-1}, across five sites. Normalized F_{cos}/NEE was 3.2±1.8, consistent with expectations (3,5,9), and with the mean ratio of 5.3±0.24 calculated from seasonal drawdowns in atmospheric COS vs. CO_2 across 12 Northern Hemisphere stations over 6-12 years. COS could be implemented within the existing global flux measurements networks and provide independent constraints on GPP estimates, which are key to projecting the land biosphere response to climate change.

Carbonyl sulfide (COS) is the sulfur-containing analog of carbon dioxide and has physical and chemical properties similar to CO_2. It is present in the atmosphere at mixing ratios of about 500 pmol mol^{-1} (parts per trillion), and is routinely measured to high precision in flask samples from surface stations and airplane profiles (4). The atmospheric chemistry of COS has been extensively investigated, as it is thought to be the major precursor of sulfur containing aerosols in the stratosphere (12). The major source to the atmosphere is via oxidation of other sulfur containing molecules in the atmosphere (CS_2 and DMS) and direct emission from the upper ocean (organic matter). The major sinks are uptake by plants and soils, and oxidation in the stratosphere. As a result of these processes the lifetime of COS in the atmosphere is 2-4 years (4,13). Studies of COS

in terrestrial ecosystems (*e.g.* 8,14,15,16 and references therein) indicate that both COS and CO_2 fluxes into leaves and soils are influenced by the same physical limitations along the diffusion pathway, followed by hydration reactions catalyzed by the enzyme carbonic anhydrase (CA). The hydration reaction is irreversible for COS (17) making it, together with the lack of any significant terrestrial production process, essentially a one-way flux into the land biosphere:

$$COS + H_2O \rightarrow H_2S + CO_2 \quad (1)$$

The possibility that COS flux could be used as a proxy for photosynthetic CO_2 uptake (18-20) is especially attractive because it is impossible to directly measure this CO_2 flux at scales above the leaf. The simultaneous occurrence of respiration from non-photosynthetic parts of plants and soil microorganisms partially offsets the photosynthetic CO_2 uptake in fields and forests. Ecosystem and local eddy covariance studies can therefore only resolve the net CO_2 exchange (NEE; 21).

The COS approach relies on a few key assumptions (co-diffusion, but no interactions, with CO_2; one-way COS flux; and negligible competing fluxes; see ref. 5) that once met allow a direct estimate of GPP at the flux tower scale according to (3,5,8):

$$GPP = \frac{F_{COS}}{LRU} \cdot \frac{C_{a-co2}}{C_{a-cos}} \quad (2)$$

where F_{COS} is the directly measured flux of COS, $C_{a\text{-}COS}/C_{a\text{-}CO2}$ is the ratio of ambient mixing ratios of COS and CO_2 used to normalize GPP and F_{cos} to their respective mixing ratios, and LRU is the leaf-scale normalized COS to CO_2 uptake (3,6,8) recently estimated to be about 1.6 (7). Ecosystem-scale relative uptake, ERU (recently estimated to be ~4; ref. 5), can also be defined based on net ecosystem CO_2 exchange, NEE, according to:

$$ERU = \frac{F_{COS}}{NEE} \cdot \frac{C_{a-cos}}{C_{a-co2}} \quad (3)$$

Even broader in scale, an atmospheric relative uptake, ARU (estimated to be ~6; ref. 4), at the local to continental scales can be used to examine the influence of vegetative uptake on the amplitude of the seasonal variations of atmospheric COS and CO_2 (or on vertical gradients observed only over terrestrial ecosystems; 3,4):

$$ARU = \frac{COS_{spring\ max} - COS_{fall\ min}}{CO2_{spring\ max} - CO2_{fall\ min}} \cdot \frac{COS_{annual\ mean}}{CO2_{annual\ mean}} \quad (4)$$

It is generally recognized that the amplitudes of seasonal CO_2 mixing ratio variations throughout the Northern Hemisphere are determined largely by seasonal changes in terrestrial NEE (22).

Here we directly explore the links between COS and ecosystem GPP by attempting the first simultaneous eddy covariance flux measurements of both COS (F_{cos}) and CO_2 (NEE) at the ecosystem scale. We carried out five field campaigns in three pine-forests along a steep precipitation gradient (290 to 720 mm annual precipitation), and in a summer and winter crop fields (cotton and

wheat respectively). We used a specially designed mobile laboratory that included an eddy covariance (EC) system centered on a fast (20 Hz) CO_2/H_2O infrared gas analyzer (IRGA) and a 3D sonic anemometer mounted on a pneumatic mast (4-28 m). The system was complemented by a quantum cascade laser (QCL) system capable of measuring COS and CO_2 at 1 Hz (10) housed in the temperature controlled lab with air sampling from an intake adjacent to the anemometer. Deployment of the mobile system was made in consideration of the EC methodology requirements established for permanent flux sites (23), such as relatively flat terrain with air sampling within the canopy mixed boundary layer.

Background mixing ratios of CO_2 and COS were on average 391±1.5 μmol mol^{-1} and 500±11 pmol mol^{-1} respectively, with little diurnal variations during the campaigns (see Fig. 1 for a typical day). These levels are consistent with the background records for this latitude (http://www.esrl.noaa.gov/gmd/), and the local station in the global observation records (http://www.weizmann.ac.il/GGI/). The small diurnal variations presumably indicated that rigorous atmospheric mixing overwhelmed any local vegetation effect in mixing ratio.

Canopy EC flux measurements showed that all sites were sinks for both CO_2 and COS with typical daily cycles peaking around mid-day (Fig. 1). As indicated above, NEE measurements were based simultaneously on two analyzers (fast IRGA and the slower QCL system), and the comparison between them (Fig. 1) indicated <10% loss of flux in the slow rate measurements, and often near zero. This provided confidence in the COS flux measurements that were only obtainable with the 1 Hz QCL measurements. We also note that while each campaign lasted over a week, the challenges associated with setting up the new and demanding COS measurements at each site, together with variations in weather conditions significantly reduced the number of complete daily cycles. The data across each campaign were consistent but we focus our site comparison here on the most complete and representative day for each campaign (see Fig. 2).

Midday NEE ranged between -3.9 and -20.4 μmol $m^{-2}s^{-1}$ and peak F_{COS} ranged between -50 and -90 pmol $m^{-1}s^{-1}$, in the dry forest and the cotton field (during the leaf expansion stage). As expected, nighttime NEE showed small positive fluxes reflecting ecosystem respiration (2.6±1.4 μmol $m^{-2}s^{-1}$, on average across sites). The nighttime F_{COS} signal was characterized by relatively low signal/noise ratio, averaging across sites at +3.9±8.6 pmol $m^{-2}s^{-1}$, emission rates that corresponded to ~6% of the mean midday uptake rates. The nighttime flux rates, however, were in most cases within the instrumental noise level. To further constrain the soil contribution to F_{COS}, several soil cores (~15

cm deep) were collected near the medium-precipitation forest site and on the Weizmann campus. The cores were sealed in specially constructed gas exchange chambers, similar to the leaf gas exchange chambers used previously (6), and gas exchange measurements were conducted. The results indicated a mean uptake rate across cores and measurement conditions of -6.6 pmol COS $m^{-2}s^{-1}$, which is within the range of -0.2 to -13.3 pmol $m^{-2}s^{-1}$ previously reported (15,16,24,25). The combined records of soil cores and field data (mean values of -6.6and +3.9 pmol COS $m^{-2}s^{-1}$) indicate soil fluxes much smaller than daytime uptake and possibly near zero, but further work with increased precision is clearly required to more precisely quantify this component.

Using equation 2 and the proposed mean LRU of 1.6 (6), we estimated GPP (GPP_{COS}) on an hourly basis at all sites (Fig. 2) and report them as daytime mean values, and daily sums (Table 1). These estimates were compared with GPP estimated by a widely used indirect approach based on nighttime NEE (when turbulence permits) representing ecosystem respiration (Re), which is, in turn, extrapolated to daytime values by applying temperature corrections. GPP_{Re} is then obtained from GPP=NEE+Re (11). Both approaches have limitations and neither one can serve as a reference (see ref. 5 for recent discussion). But GPP_{COS} measurements offer a direct approach, not based on extrapolated value. Notably, the limitations of our 'first generation' COS measurements are rapidly being overcome as new, higher precision QCL instruments are currently being developed. Nevertheless, we estimate magnitudes for GPP based on COS fluxes (GPP_{COS}) at all sites and along the climate gradient that are comparable to those from the more traditional methodology (GPP_{Re}). In all cases GPP estimates from both methods show similar daily cycles (Fig. 2), and values that agree to within ±20% on average (better than ±10% excluding the low activity dry pine forest). Note that the GPP_{COS} values were not adjusted for possible soil contributions. We justify this given the inconclusive and near zero nighttime and soil chamber measurements noted above. But we realize that on average GPP_{COS} values were slightly higher than GPP_{Re} (by ~3% based on daily sums, without considering the unusual dry forest site; Table 1), which may result from some soil COS uptake (i.e. daytime soil COS uptake would enhance F_{COS} and consequently GPP_{COS}).

An uncertainty in the application of the COS/CO_2 approach presented here may be introduced by the use of a constant LRU value (1.6; ref. 6). LRU reflects first the physical distinctions between COS and CO_2 (e.g. mass, diffusivity), and secondly, small differences in the transport pathway from the ambient atmosphere to the site of the biochemical enzyme reaction in the leaves, and possibly reaction rates (7,9,26). A review of the factors that can potentially contribute to variations in LRU was recently made (27), but the results of the survey across a wide range of plant species and

functional groups (7), and the good agreement of GPP_{COS} vs GPP_{Re} reported here may indicate that in reality, these effects have a relatively small influence on estimates of GPP over daily or longer periods. Possibly the major contribution to variations in LRU is changes in the internal conductance (g_m) to COS and CO_2 (9,26). It is generally assumed that stomatal conductance (g_s) dominates the diffusion of both COS and CO_2 into leaves, with g_s/g_m of ~0.2, as confirmed in lab experiments (6). However, under environmental stress or across plant species, internal conductance, g_m, may decrease. This effect is likely to be greater for CO_2 with its longer path to the site of carboxylation in the chloroplast, compared with COS hydrolyzed by the enzyme carbonic anhydrase (CA; see eq. 1) that may be closer to the gas-air interface. In variable field conditions higher g_s/g_m and consequently higher LRU values may be expected. This perspective is significant because it indicates that LRU may vary mostly upwards compared to the mean value reported (7,9,26,27). The sensitivity of inferred GPP_{COS} to the LRU value used exhibits a power-law type behavior (Figure 2c), indicating that GPP_{COS} has a low sensitivity to variations in LRU values above the observed mean value of 1.6. This gives some robustness to the GPP_{COS} estimates that rely on this mean value for LRU.

Estimating ecosystem relative uptake (ERU; eq. 3) based either on the daily sums of F_{COS} and NEE or the daytime mean values (about 9:00 to 17:00) for each site indicated a mean ERU of about 3.2 in both cases. This value is consistent with the expected values reported based on less direct approaches of 2.8-4.3 (3,5,9). A somewhat higher ERU value of ~6 was observed in our dry forest site. This site, however, is characterized by a relatively extensive biological soil crust (composed of algae, mosses and lichens, common in arid regions; 28,29), which could enhance the soil uptake of COS and consequently ERU. More detailed examination of biological soil crust effects over the diurnal cycle is recommended. Combining equations 2 and 3 yield ERU/LRU=GPP/NEE. The mean daytime ERU value we derive of 3.2 suggests therefore a mean daytime GPP/NEE of 2. Including nighttime NEE in calculating ERU increases the mean, diurnally based ERU to 4.9 and implies a mean GPP/NEE value for our sites of 3.1, which is similar to accepted values (30). Finally, as noted above, high precision measurements of atmospheric COS are performed routinely at now 15 sampling sites around the world, with a duration of up to twelve years at some sites (a continuation of work in ref. 4). Combining this record with the CO_2 measurements (http://www.esrl.noaa.gov/gmd/) for the same sites, we obtained a robust estimate of ARU (eq. 4, Fig. 3a) of 5.3±0.24, which is somewhat lower than the first estimate made with fewer data (4), but consistent with the ecosystem values observed in this study (and with vertical gradients above ecosystems; 3,4). Excluded from this ARU estimates are the Southern Hemisphere sites (with little effect), and a few data points from Wisconsin that are clearly distinct that may reflect local effects

of intensive agriculture and have mean ARU of 3.5±02, more characteristics of our ERU (Table 1). Considered together, the concentration and flux measurements of COS presented here show that the evolution of the COS/CO_2 relative uptake can be accurately traced from the leaf, through the ecosystem to the continental scale, as demonstrated schematically in Fig. 3b. Note that in the global atmospheric scale, an alternative to COS to asses the net vs. gross CO_2 exchange fluxes with the biosphere does not exist (unlike the GPP_{Re} option at the ecosystem scale).

The encouraging results of COS/CO_2 approach and the newly available analytical means to incorporate it into traditional flux measurements could result in new independent estimates of GPP and constitutes a breakthrough in our ability to understanding terrestrial carbon fluxes and in projecting the land biosphere response to global change.

Methods

Five field campaigns of 7-14 days each were carried out during 2011-2012 (one during summer 2011 the rest during the winter/spring local active period). Three of the campaigns were carried out in pine forests (predominantly *Pinus halepensis*) along the precipitation gradient in Israel: Dry site (31° 20' 49.2" N 035° 03' 07.2" E; precipitation 280 mm), which is a permanent flux site (31) and allowed an inter-comparison of flux measurements between the permanent and mobile flux systems); intermediate site (31° 47' 34.5" N 035° 00' 11.5" E; precipitation 520 mm); wet site in Northern Israel (33° 00' 00.5" N 035° 30' 40.5" E; precipitation 710mm). Two campaigns in crop fields: Cotton field during summer and peak leaf expansion (31° 50' 51.5" N 034° 46' 34.2" E; irrigation 550mm); wheat field during winter (31° 53' 07.1" N 034° 53' 09.2" E; irrigation 540mm). A newly designed mobile flux measurement system was used in all campaigns, based on 12 ton 4x4 truck 30 m pneumatic mast and complete eddy flux system. The lab provided air-conditioned instrument facility (cellular communication, 18 KVA generator, 4200W UPS). Flux, meteorological, and radiation measurements rely on an eddy-covariance (EC) system that provides CO_2, sensible and latent heat fluxes using 3D sonic anemometer (R3, Gill Instruments, UK) and closed-path CO_2/H_2O infrared gas analyzer (Li-Cor 7200) using CarboEuroflux methodology (23), and EddyPro Software (www.licor.com/). Air temperature and relative humidity (HMP45C probes, Campbell Scientific) and air pressure (Campbell Scientific sensors) were measured ~3 m above the canopy. Energy fluxes rely on radiation sensors including solar radiation (0.29-4.0 μm; CMP21, Kipp&Zonen); longwave radiation (4.0-100 μm; CRG4, Kipp&Zonen); and photosynthetic radiation (PAR, 0.4-0.7 μm; PAR-LITE2). All sensors are installed in pairs facing up and down, and they are connected using differential mode via a multiplexer to a data logger (Campbell Scientific). A mid IR dual-Quantum Cascade Laser spectrometer (QCL- Aerodyne Research Inc., Billerica, MA) was utilized to measure COS and CO_2 concentrations at a 2056 cm^{-1} with a thermoelectrically cooled detector as described previously by Stimler et al., (10), at a rate of 1Hz. The inlet tube of the measurements was installed next to a sonic anemometer. A calibration gas mixture for COS was obtained from NOAA-GMD (4), CO_2 was calibrated

against lab tanks that undergo periodic inter-comparison with the NOAA-GMD lab. We computed 30-min and 60-min mean fluxes using Eddy-pro 3.0 software. The ratio of the 20 Hz fluxes of CO_2 from the Li-Cor to the 1 Hz measurements of the Li-Cor and the QCL for each 30-min interval provided an estimate of flux loss by instrumental smoothing of high-frequency fluctuations (33; Fig. 1). GPP for each site was estimated via eq. 2, and using the conventional approach of estimating ecosystem respiration (Re). The latter was carried out using a regression of NEE on turbulent nights against temperature, followed by extrapolating the derived nighttime Re-temperature relationship to daytime periods and the relationship: GPP = NEE+Re (11). Atmospheric mixing ratio for both COS and CO_2 were obtained by NOAA-GMD global observations network (www.esrl.noaa.gov/gmd) as described in detail in Ref. 4.

References

1. Raupach, M. R. Pinning down the land carbon sink. *Nature Climate Change* **1,** 148-149 (2011).
2. Pan, Y. *et al*. A Large and Persistent Carbon Sink in the World's Forests. *Science* **333**, 988-993 (2011).
3. Campbell, J. E. *et al*. Photosynthetic control of atmospheric carbonyl sulfide during the growing season. *Science* **322**, 1085-1088 (2008).
4. Montzka, S. A. *et al*. On the global distribution, seasonality, and budget of atmospheric carbonyl sulfide (COS) and some similarities to CO_2. *J. Geophys. Res.* **112**, 9302-9317 (2007).
5. Blonquist, J. M. *et al*. The potential of carbonyl sulfide as a proxy for gross primary production at flux tower sites. *J. Geophys. Res.* **116**, 4019-4037 (2011).
6. Stimler, K., Montzka, S., Berry, J. A,, Rudich, Y. & Yakir, D. Relationships between carbonyl sulfide (COS) and CO_2 during leaf gas exchange. *New Phytology*, **186**, 869-978 (2010)**.**
7. Stimler, K., Berry, J. A. & Yakir, D. Variations in leaf COS/CO2 uptake across species and a possible COS mediated H2S effect on stomatal conductance. *Plant Physiol*. **158**, 524-530 (2011).
8. Sandoval-Soto, L. *et al*. Global uptake of carbonyl sulfide (COS) by terrestrial vegetation: Estimates corrected by deposition velocities normalized to the uptake of carbon dioxide (CO_2), *Biogeosciences*, **2**, 125-132 (2005).
9. Seibt, U., Kesselmeier, J., Sandoval-Soto, L., Kuhn, U., & Berry, J. A. A kinetic analysis of leaf uptake of COS and its relation to transpiration, photosynthesis and carbon isotope fractionation. *Biogeosciences*, **7**, 333-341 (2010).
10. Stimler, K., Nelson, D. & Yakir, D. High precision measurements of atmospheric concentrations and plant exchange rates of Carbonyl Sulfide (COS) using mid-IR Quantum Cascade Laser. *Glo. Chan. Bio.*, **16**, 2496-2503 (2010).

11. Reichstein, M. *et al*. On the separation of net ecosystem exchange into assimilation and ecosystem respiration: Review and improved algorithm. *Global Change Biol*., **11**, 1424–1439 (2005).
12. Bruhl, C., Lelieveld, J., Crutzen, P. J. & Tost H. The role of carbonyl sulphide as a source of stratospheric aerosol and its impact on climate. *Atmos. Chem. Phys*., **12**, 1239-1253 (2012).
13. Kettle, A. J. *et al*. Comparing forward and inverse models to estimate the seasonal variation of hemisphere-integrated fluxes of carbonyl sulfide. *Atmos. Chem. Phys*., **2**, 343–361 (2002).
14. Yonemura, S. *et al*. COS uptake and DMS emission by/from plants. *Phyton*,**45**, 17-24 (2005).
15. Kesselmeier, J., Teusch, N., & Kuhn, U. Controlling variables for the uptake of atmospheric carbonyl sulfide (COS) by soil, *J. Geophys. Res.-Atmos*., **104**, 11577–11584 (1999).
16. Steinbacher, M., Bingemer, H. G. & Schmidt, U. Measurements of the exchange of carbonyl sulfide (OCS) and carbon disulfide (CS2) between soil and atmosphere in a spruce forest in central Germany, *Atmos. Environ*., **38**, 6043–6052 (2004).
17. Protoschill-Krebs, G., & Kesselmeier, J. Enzymatic pathways for the metabolization of carbonyl sulphide (COS) by higher plants, *Bot. Acta*, **108**, 445–448 (1992).
18. Bartell, U. *et al*. COS and H_2S fluxes over a wet meadow in relation to photosynthetic activity: An analysis of measurements made on 6 September 1990. *Atmos. Environ*., **27A**, 1851–1864 (1993).
19. White, M. L. *et al*. Carbonyl sulfide exchange in a temperate loblolly pine forest grown under ambient and elevated CO_2. *Atmos. Chem. Phys*., **10**, 547–561 (2010).
20. Xu, X., Bingemer, H. G. & Schmidt, U., The flux of carbonyl sulfide and carbon disulfide between the atmosphere and a spruce forest*, Atmos. Chem. Phys*., **2**, 171–181 (2002).
21. Baldocchi, D. *et al*., FLUXNET: A new tool to study the temporal and spatial variability of ecosystem-scale carbon dioxide, water vapor, and energy flux densities. *Bull. Am. Meteorol. Soc.*, **82**, 2415–2434 (2001).
22. Randerson. J.T., et al., The contribution of terrestrial sources and sinks to trends in the seasonal cycle of atmospheric carbon dioxide. *Global Biogeochem. Cycles*, **4**, 535-560 (1997).
23. Aubinet, M., Vesala, T. & Paple, D. *Eddy Covariance: A practical guide to measurement and data analysis Ch. 2* (Springer, New York, 2012).
24. Kuhn, U. *et al*. Carbonyl sulfide exchange on an ecosystem scale: soil represents a dominant sink for atmospheric COS. *Atmos. Environ*., **33**, 995–1008 (1999).
25. Yi, Z. *et al.* Soil uptake of carbonyl sulfide in subtropical forests with different successional stages in south china. *J. Geophys. Res.-Atmos*., **112**, 8302–8313 (2007).

26. Seibt, U., Rajabi, A., Griffiths, H. & Berry, J. A. Carbon isotopes and water use efficiency: sense and sensitivity. *Oecologia*, **155**, 441–454 (2008).
27. Wohlfahrt, G. *et al.* Carbonyl sulfide (COS) as a tracer for canopy photosynthesis, transpiration and stomatal conductance: potential and limitations. *Plant, Cell and Envir.,* **35**, 657-667 (2012).
28. Gelfand, I., Grunzweig, J. M. & Yakir, D. Slowing of nitrogen cycling and increasing nitrogen use efficiency following afforestation of semi-arid shrubland. *Oecologia*, **168**, 563-575 (2012).
29. Wilske, B. *et al.* The CO_2 exchange of biological soil crusts in a semiarid grass-shrubland at the northern transition zone of the Negev desert, Israel. *Biogeosciences*, **5**, 1411-1423 (2008).
30. Falge E. *et al.* Seasonality of ecosystem respiration and gross primary production as derived from FLUXNET measurements. *Agri. Forest Meteor.* **113**, 53-74 (2002).
31. Grunzweig, G. M., Lin, T., Rotenberg, E., Schwartz, A. & Yakir, D. Carbon sequestration in arid-land forest. *Glo. Chan. Bio.*, **9**, 791-799 (2003).
32. Nelson, D., McManus, B., Urbanski, S., Herndon, S. & Zahniser, M.S. High precision measurements of atmospheric nitrous oxide and methane using thermoelectrically cooled mid-infrared quantum cascade lasers and detectors. *Spectrochimica Acta*, **60**, 3325–3335 (2004).
33. Goulden, M. L., Munger, J. W., Fan, S.M., Daube, B. C. & Wofsy, S. C. Measurements of carbon sequestration by long-term eddy covariance: Methods and a critical evaluation of accuracy, *Global Change Biol*., **2**, 169–182 (1996).

Table 1. Atmosphere-vegetation exchange fluxes of CO_2 and COS in five field campaigns.

	NEE [mmol $m^{-2}d^{-1}$]	F_{COS} [µmol $m^{-2}d^{-1}$]	ERU Daytime	GPP	
				GPP_{COS}	GPP_{Re}
		Daytime Sum			
	[mmol m^{-2} d^{-1}]	[µmol m^{-2} d^{-1}]		[mmol m^{-2} d^{-1}]	[mmol m^{-2} d^{-1}]
Cotton	-519	-2151	3.3	1042	940
Wheat	-455	-1260	2.1	630	621
Pine - 280	-119	-927	6.2	423	150
Pine - 520	-396	-1288	2.4	582	579
Pine – 710	-481	-1364	2.1	609	601
Average:	**-394±160**	**-1398±453**	**3.2±1.8**	**657±230**	**578±281**
		Daytime Mean			
	[µmol m^{-2} s^{-1}]	[pmol m^{-2} s^{-1}]		[µmol m^{-2} s^{-1}]	[µmol m^{-2} s^{-1}]
Cotton	-14.4±8.1	-59.8±29.4	3.3±0.4	32.9 ±12.2	27.1 ± 7.8
Wheat	-11.6±7.1	-36.3±18.6	2.3±0.9	18.0±8.5	15.8±8.0
Pine - 280	-3.3±1.8	-25.9±9.5	6.3±2.6	12.8±3.4	4.5±1.2
Pine - 520	-11.0±4.3	-35.8±18.5	2.4±0.9	14.0±8.9	14.9±6.3
Pine – 710	-13.4±4.4	-37.9±19.5	2.1±1.1	16.9±8.5	16.7±4.5
Average:	**-10.7±4.4**	**-39.1±12.5**	**3.3±1.7**	**18.9±8.1**	**15.8±8.0**

Flux measurements of COS and CO_2 in five field campaigns. Fluxes of CO_2 and COS measured above the canopy by the eddy covariance technique in Israel in winter crop (wheat), summer crop (cotton) and three pine forests along precipitation gradient (mean annual precipitation indicated). Net ecosystem exchange of CO_2 (NEE) and COS (F_{cos}) are reported as daytime sum and mean values for around 9:00-17:00 for a representative day during each campaign. Ecosystem relative uptake was obtained from the ratio of F_{cos}/NEE normalized by the respective ambient mixing ratio (~390 mmol mol^{-1} for CO_2 and ~500 pmol mol^{-1} for COS). GPP_{COS} was obtained form F_{COS} and the ambient mixing ratios using equation 2. GPP_{RE} was obtained using nighttime NEE (11). Standard error of the mean is indicated when appropriate. For the daytime mean values, this reflects the variations in fluxes along the day.

Figure Captions

Figure 1. Diurnal cycles in atmospheric mixing ratios and atmosphere-vegetation exchange fluxes of CO_2 and COS. Typical diurnal cycles in (a) the atmosphere-vegetation COS flux (F_{COS}) above a cotton field, and in the atmospheric COS mixing ratios (pmol mol^{-1}; ppt) ~3 m above the vegetation canopy, and (b) in the atmospheric CO_2 mixing ratios (µmol mol^{-1}) the net ecosystem CO_2 exchange (NEE; µmol $m^{-2}s^{-1}$) measured both in the 20Hz infrared gas analyzer and the 1 Hz quantum cascade laser, with the later used also for F_{COS}. Flux loss (underestimated) due to the slow measurements was <10% and often near zero.

Figure 2. Diurnal cycles in photosynthetic gross primary productivity (GPP). (a,b,d,e) Typical diurnal cycle in GPP in two crop fields (winter wheat, summer cotton) and three pine forests along a

precipitation gradient (mean annual precipitation, 280, 520, 710 mm, is indicated). GPP_{COS} was estimated directly from eddy covariance measurements of COS (F_{COS}, equation 2 using LRU=1.6; 7), or indirectly (11) based on nighttime NEE measurements extrapolated to daytime to account for ecosystem respiration (Re, GPP_{Re}). (f) Average sensitivity of the GPP estimates to LRU value used in GPP_{COS} estimates, indicating the relative robustness associated with variations of LRU above the mean value of 1.6.

Figure 3. Relative uptake of COS vs. CO_2. (a) Atmospheric relative uptake (ARU; equation 4; c.f. ref. 4) of COS vs. CO_2 obtained from the slope (model II linear regression) of the measured seasonal peak to peak (winter/spring – summer/fall) draw-down of these two trace gases across 15 sampling Northern Hemisphere stations with up to 12 years of data, with each data point representing one year, one station (n=147; Southern Hemisphere station, full circles, distinct data from Wisconsin USA, squares, with mean ARU value of 3.5±0.2, probably reflecting local effects of intensive agriculture, and three extreme outliers from different sites and times, were excluded from the regression). The observed ARU=5.3±0.2 is consistent with the ecosystem-scale, ERU, values reported in Table 1 and the schematic in (b), which indicates the increasing COS/CO_2 flux ratio along the cascade of respiratory processes that diminishes the net CO_2 flux, but not that of COS.

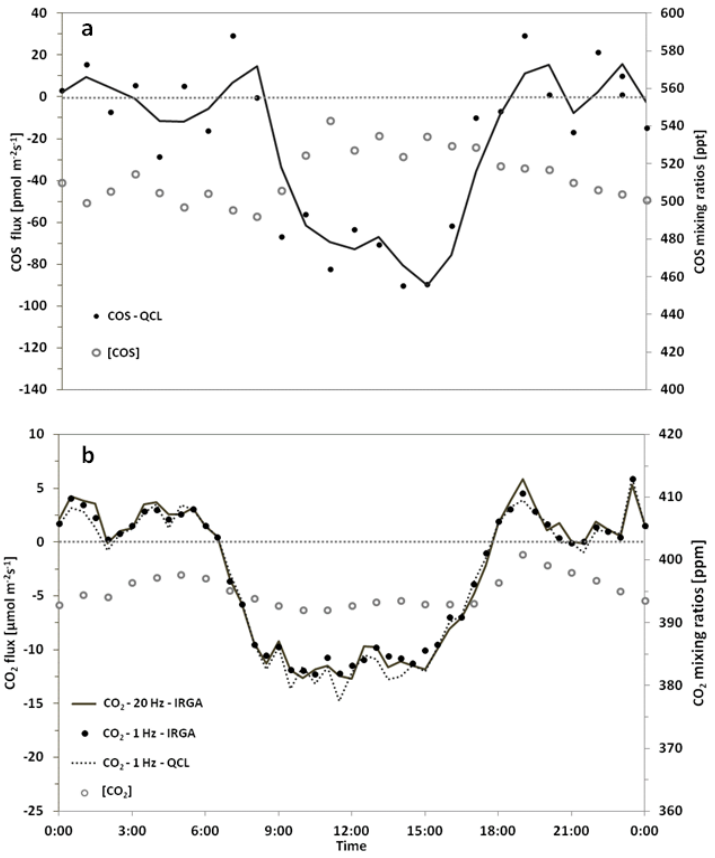
a
COS flux [pmol m-2s-1]
COS mixing ratios [ppt]
COS - QCL
[COS]
b
CO2 flux [µmol m-2s-1]
CO2 mixing ratios [ppm]
CO2 - 20 Hz - IRGA
CO2 - 1 Hz - IRGA
CO2 - 1 Hz - QCL
[CO2]
Time

Fig. 1

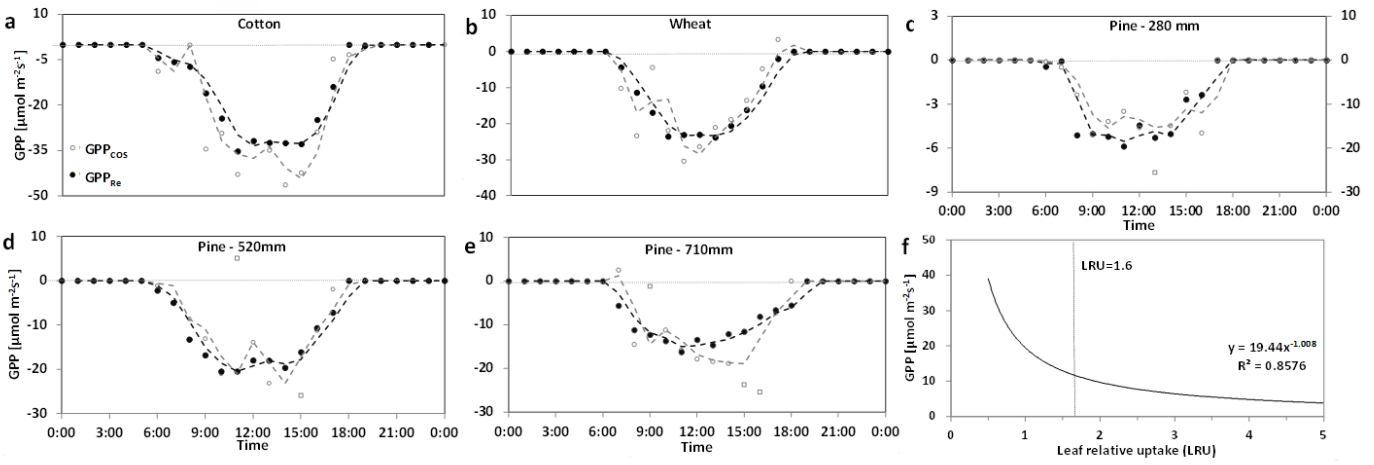
a
Cotton
GPP [µmol m-2s-1]
GPPcos
GPPRe
b
Wheat
c
Pine - 280 mm
Time
d
Pine - 520mm
e
Pine - 710mm
f
LRU=1.6
y = 19.44x-1.008
R² = 0.8576
Leaf relative uptake (LRU)

Fig. 2

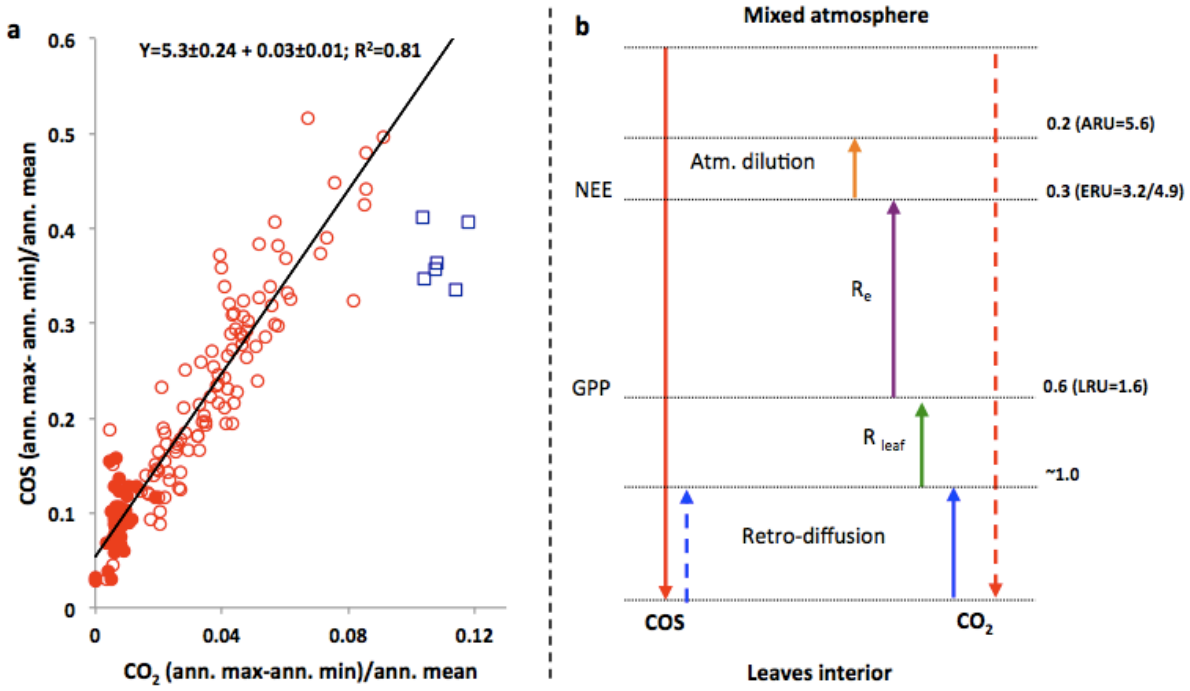
a
Y=5.3±0.24 + 0.03±0.01; R²=0.81
COS (ann. max- ann. min)/ann. mean
CO2 (ann. max-ann. min)/ann. mean
0
0.1
0.2
0.3
0.4
0.5
0.6
0.04
0.08
0.12
b
Mixed atmosphere
0.2 (ARU=5.6)
Atm. dilution
NEE
0.3 (ERU=3.2/4.9)
Re
GPP
0.6 (LRU=1.6)
R leaf
~1.0
Retro-diffusion
COS
CO2
Leaves interior

Fig. 3